Journal of Hazardous Materials 170 (2009) 754–762

Contents lists available at ScienceDirect

Journal of Hazardous Materials

journal homepage: www.elsevier.com/locate/jhazmat

Effect of the adsorbate (Bromacil) equilibrium concentration in water on its adsorption on powdered activated carbon. Part 2: Kinetic parameters

Fadi Al Mardini [1], Bernard Legube *

Université de Poitiers, CNRS, Laboratoire de Chimie et Microbiologie de l'Eau (UMR 6008), Ecole Supérieure d'Ingénieurs de Poitiers, 40 avenue du Recteur Pineau, 86022 Poitiers Cedex, France

ARTICLE INFO

Article history:
Received 9 February 2009
Received in revised form 18 May 2009
Accepted 19 May 2009
Available online 22 May 2009

Keywords:
Adsorption
Kinetic
Water
Powdered activated carbon
Bromacil

ABSTRACT

The application of several monosolute equilibrium models has previously shown that Bromacil adsorption on SA-UF (Norit) powdered activated carbon (PAC) is probably effective on two types of sites. High reactivity sites were found to be 10–20 less present in a carbon surface than lower reactivity sites, according to the q_m values calculated by isotherm models. The aims of this work were trying, primarily, to identify the kinetic-determinant stage of the sorption of Bromacil at a wide range of initial pesticide concentrations (~5 to ~500 μg L^{-1} at pH 7.8), and secondly, to specify the rate constants and other useful design parameters for the application in water treatment. It was therefore not possible to specify *a priori* whether the diffusion or surface reaction is the key step. It shows that many of the tested models which describe the stage of distribution or the surface reaction are correctly applied. However, the diffusivity values (D and D_0) were found to be constant only constants for some specific experimental concentrations. The HSDM model of surface diffusion in pores was also applied but the values of the diffusion coefficient of surface (D_s) were widely scattered and reduce significantly with the initial concentration or the equilibrium concentration in Bromacil. The model of surface reaction of pseudo-second order fitted particularly well and led to constant values which are independent of the equilibrium concentration, except for the low concentrations where the constants become significantly more important. This last observation confirms perfectly the hypothesis based on two types of sites as concluded by the equilibrium data (part 1).

1. Introduction

Sorption at the interface liquid/solid, with a localized reaction in the pores (of adsorbents, ion exchangers, catalysts, etc.), is generally described by three major steps [1] in perfectly mixed system:

- the diffusion through the film surrounding the solid adsorbent particles, called also "external diffusion";
- the diffusion in the pores of the adsorbent or "intra-particle diffusion";
- the reaction of adsorption (and desorption) itself or "surface reaction".

One (or more) of these steps can be kinetically decisive. The surface reaction is usually a quick step; some authors [2,3] consider that only the intra-particle diffusion govern the sorption kinetics. Desorption, when it occurs significantly (K_L low, $n_{Freundlich} > 1$), presents the same steps in reverse order.

Several equations are used for external diffusion [4,5]. This step is not often decisive, especially when the experimental system is well agitated.

According to the initial work of Weber and Morris [6], the kinetic expression of intra-particle diffusion is often presented by a linear variation of the concentration of adsorbate with the square root of the contact time, whose slope is equivalent to the rate constant [7–12]. Other models of intra-particle diffusion have been developed and used. Their development was based on the ancient works of Boyd et al. [13] and Vermeulen [14] or more recent works of Mathews and Weber [15] for the theory of "Homogeneous Solid Phase Diffusion Model". These approaches can determine several types of diffusivity coefficients.

Regarding the step of "surface reaction", the classic expressions of pseudo-first-order (so-called "Largergren") [16] and pseudo-second-order kinetic models are often tested [9,17–22]. When the desorption step is also taken into account, a kinetic expression so-called "Langmuir" [22] or "Adams–Bohart–Thomas" [8] is sometimes used.

Some other general expressions can be found in the literature, such as "Bangham" [9,23] or "Statistic Rate Theory"

* Corresponding author. Tel.: +33 5 49453917; fax: +33 5 49453768.
E-mail addresses: almardinifadi@yahoo.fr (F. Al Mardini), Bernard.legube@univ-poitiers.fr (B. Legube).
[1] University of Damascus, Faculty of Sciences, Department of Chemistry, Al Baramkeh, Damascus, Syria.

0304-3894/$ – see front matter © 2009 Elsevier B.V. All rights reserved.
doi:10.1016/j.jhazmat.2009.05.087

Nomenclature

a/V or S_s	specific area of the solid / liquid interface
A_0, A_1, A_2, ...	parameters that describe the mathematical solution (from HSDM model)
C_e	Bromacil concentration at equilibrium ($mg\,L^{-1}$, $\mu g\,L^{-1}$)
C_0	initial Bromacil concentration ($mg\,L^{-1}$, $\mu g\,L^{-1}$)
C_t	solute concentration at each time t in the aqueous phase ($mg\,L^{-1}$)
C^*	$C^* = (C_t - C_e)/(C_0 - C_e)$ (from HSDM model)
D	diffusivity (from Vermeulen) ($m^2\,s^{-1}$)
D_s	surface-diffusion coefficient (from HSDM model) ($m^2\,s^{-1}$)
D_0	diffusivity (from Rudzinski and Plazinski) ($m^2\,s^{-1}$)
DOC	dissolved organic carbon ($mg\,L^{-1}$)
F_t	reaction advancement
k_{ads}	rate constant of adsorption ($L\,mg{-}1\,min^{-1}$)
k_{des}	rate constant of desorption (min^{-1})
k_f	transfert external coefficient (from Furusawa and Smith) ($m\,min^{-1}$)
K_L	Langmuir- or Tóth-isotherm constant
k_V	diffusion constant of intra-particular (from Vermeulen) (min^{-1})
k_W	diffusion constant of intra-particular (from Weber et Morris) ($m\,L^{-1}\,min^{-0.5}$)
k_{1app}	rate constant of pseudo-first order (min^{-1})
k_{2app}	rate constant of pseudo-second order ($L\,mg^{-1}\,min^{-1}$)
m	PAC mass (g)
$m_s = m/V$	PAC concentration ($g\,L^{-1}$)
n	Tóth-isotherm constant
PAC	powdered activated carbon
q_e	PAC-surface-complex concentration at equilibrium ($mg\,g^{-1}$)
q_m	Langmuir-maximum adsorption capacity ($mg\,g^{-1}$)
q_t	PAC-surface-complexe concentration at time t ($mg\,g^{-1}$)
R_a	radius of adsorbent (supposed spherical) (m)
S_s	specific area of adsorbent (or a/V) (m^{-1})
V	solution volume (L)

Greek letter

θ	surface coverage (q_e/q_m)

[23–27] which describes the rate of the reaction adsorption/desorption.

Most of the studies on the adsorption kinetics of a chemical compound in aqueous solution are generally conducted for narrow ranges of initial chemical compound and adsorbent concentrations, even sometimes on the basis of a single initial concentration and/or adsorbent.

In our study the application of several monosolute equilibrium isotherm models generally revealed [28] that the adsorption of an adsorbate (Bromacil) probably occurs on two types of activated carbon site (PAC Norit SA-UF). At very low adsorbate concentration (<10 $\mu g\,L^{-1}$ in our case), these are high reactivity free sites (or pores) which react ($K_L \sim 10^3\,L\,mg^{-1}$). When the initial adsorbate concentration is higher, a large proportion of this concentration mostly adsorbs on lower reactivity free sites ($K_L \sim 10\,L\,mg^{-1}$). This second part of the study was carried out to confirm this hypothesis by applying kinetic models to assess our experimental results.

Our present work was carried out to investigate the apparent adsorption rate of Bromacil on a commercial powdered activated carbon (PAC Norit SA-UF) with very different initial Bromacil concentrations (~5 to ~400 $\mu g\,L^{-1)}$ and PAC concentrations ranging from 0.1 to 5 $mg\,L^{-1}$.

The results were interpreted in order to try to establish the key sorption step (or steps), and also to determine the values of the rate constants and other kinetic parameters by assessing their dependence on the equilibrium or initial concentration. Ten kinetic models were tested from more than 20 experiments with different initial concentrations. These data provided by this study should contribute to a better knowledge on the adsorption kinetics of a micropollutant on a PAC widely used in drinking water treatment.

2. Materials and methods

2.1. Kinetic experiments

The protocol for the equilibrium isotherm experiment [28] was also used for the kinetic experiments with two different reactors depending on the concentration ranges studied:

- an agitated and thermostated reactor with a maximum 15-L volume, for high and medium Bromacil concentrations;
- an agitated and nonthermostated reactor with a 250-L volume for very low Bromacil concentrations.

The Bromacil mother solution was prepared in ultrapure water (DOC $\leq$ 0.1 $mg\,C\,L^{-1}$). The solutions to adsorb were prepared by dilution with ultrapure water for the 15-L reactor, or reverse osmosis water (DOC = 0.1–0.12 $mg\,L^{-1}$) for the 250-L reactor. These solutions were buffered with sodium phosphate salts (NaH_2PO_4, H_2O and Na_2HPO_4), at a final ionic strength of 1.75×10^{-3} M. The pH of the final solution to study was adjusted to 7.8 ± 0.03. For plotting the adsorption kinetics, a PAC mass was introduced in the buffered Bromacil solution.

2.2. Powdered activated carbon and chemicals

Norit SA-UF powdered activated carbon was used in this study. This PAC was chosen because of its high mesopore and secondary micropore content and since it is commonly used in drinking water treatment, especially combined with ultrafiltration. The pore structure properties (PSPs) were extracted from literature (Table 1). The PSPs parameters were determined by the N_2 adsorption isotherm technique [32].

2.3. Analytical procedure

The sampling and analyses were carried out using the same protocols as in the equilibrium parameter study [28]. Before each analysis, a standard range was prepared to determine, as precisely as possible, the initial and equilibrium Bromacil concentrations using HPLC coupled with a UV detector, directly or after a preconcentration, depending on the Bromacil concentrations [28].

3. Results and discussion

3.1. General

More than 20 experiments were carried out with initial Bromacil concentrations (C_0) ranging from 5 to 400 $\mu g\,L^{-1}$. For each experiment, a PAC mass was chosen so that Bromacil adsorption would not exceed ~90% of the initial concentration. Table 2 presents these experiments, which are numbered 1–23 in decreasing order of equilibrium concentration (C_e). The results were processed in the form q_t *vs* C_t, where

Table 1
Bibliographic data on the PAC Norit SA-UF used in this study.

	PAC "SA-UF" from France [29,30]	PAC "SA-UF" from France [31]	PAC "SA-UF" from Netherlands [31]
BET surface area	1112 $m^2 g^{-1}$	1085 $m^2 g^{-1}$	1112 $m^2 g^{-1}$
Ashes	8.17%	–	–
Humidity	2%	–	–
Apparent density	0.16 g cm^{-3}	–	–
Average geometric diameter	6 μm	–	–
Volume of primary micropores (<8 Å)	0.343 $cm^3 g^{-1}$	0.226 $cm^3 g^{-1}$	0.214 $cm^3 g^{-1}$
Volume of secondary micropores (>8 Å)	0.194 $cm^3 g^{-1}$	–	–
Volume of mesopores (20–500 Å)	0.357 $cm^3 g^{-1}$	0.885 $cm^3 g^{-1}$	0.844 $cm^3 g^{-1}$
Surface area of micropores	733 $m^2 g^{-1}$	662 $m^2 g^{-1}$	615 $m^2 g^{-1}$
Surface area of mesopores	379 $m^2 g^{-1}$	423 $m^2 g^{-1}$	421 $m^2 g^{-1}$

Table 2
Experimental conditions for the adsorption kinetics of Bromacil in buffered solution (pH 7.8) on PAC Norit SA-UF.

Kinetic experiment	C_e (μg L^{-1})	C_0 (μg L^{-1})	m_s (mg L^{-1})	Time period of models application (total time followed in min)
# 1	248	362	1	5–30 (~330)
# 2	216	351	1.5	10–45 (~330)
# 3	205	400	2	7–60 (~330)
# 4	176	356	2.5	5–60 (~330)
# 5	115.5	150	0.5	5–60 (~330)
# 6	115	371	3	5–30 (~330)
# 7	94	169	1	10–60 (~330)
# 8	74	320	5	7–30 (~330)
# 9	67	145	1.5	7–30 (~330)
# 10	59	159	1.9	3–30 (~330)
# 11	57.5	80	0.5	7–30 (~330)
# 12	40	155.8	3	4–30 (~330)
# 13	28	61	1	7–30 (~330)
# 14	23	31	0.25	5–120 (~330)
# 15	17.1	30.1	0.5	5–90 (~330)
# 16	15.6	53	2.5	7–30 (~330)
# 17	12.5	66	3	10–60 (~330)
# 18	5.3	38	2	3–15 (~330)
# 19	4.3	5.5	0.1	60–480 (~10,000)
# 20	2.9	5.4	0.2	60–480 (~10,000)
# 21	2.1	5.7	0.3	5–360 (~10,000)
# 22	2.0	30.8	3	4–30 (~330)
# 23	1.4	5.1	0.4	60–540 (~10,000)

– q_t (mg g^{-1}), concentration of surface complexes at each time t;
– C_t (mg L^{-1} or μg L^{-1}), Bromacil concentration at each time t.

Figs. 1 and 2 present two examples of the results. They clearly show that the equilibrium was reached quickly, after about 2 h, for the high initial Bromacil concentrations, and after about 6 h for low concentrations. The chosen minimum time of 6 h to monitor the reaction was therefore apparently enough.

Ten of the classical kinetic models were tested in all of the experiments (only six of them are presented here, Table 3). As in standard chemical reactions, kinetic models were applied for an advancement of the reaction to not more than 80–90% of the equilibrium level: $0 < F_t = q_t/q_e < 0.8–0.9$. For simplicity, only a few kinetic interpretation examples are shown as curves, while others are summarized in table form.

3.2. Adsorption kinetics governed by diffusion steps

3.2.1. External diffusion

The two external diffusion models, Eqs. (1) and (2) (Table 2), were not suitable for our case, which was predictable given the agitation applied during the experiments.

3.2.2. Intra-particular diffusion

To test the validity of the kinetic expression for intra-particular diffusion, proposed by Weber and Morris [6], variations in q_t were plotted *vs* the square root of time (Eq. (3), Table 3). For 19 of the 23 cases studied, plotting q_t *vs* $t^{1/2}$ was suitable for $F_t \leq 0.7–0.85$. For the four other cases, the model was unsuitable (# 15) or the number of experimental points was insufficient at the beginning of the reaction (# 19, 20, and 23). However, the lines obtained levelled off for the greatest advancements of the reaction and tended towards the horizontal asymptote around equilibrium. An example is given in Fig. 3.

The rate constant values, i.e., k_W in Eq. (3), ranged from a few 10^{-2} to few 10^{-4} mg L^{-1} $min^{-0.5}$ and the $k_W/(C_0)^{0.5}$ ratio was not very constant in opposition with what was mentioned by the model designers [6].

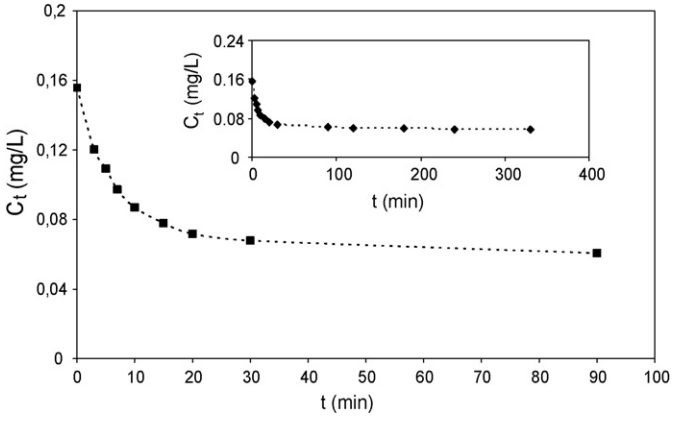

Fig. 1. Example of raw kinetics data for Bromacil adsorption on PAC Norit SA-UF at pH 7.8 (# 10, C_0 = 159 μg L^{-1} and m_s = 2 mg L^{-1}).

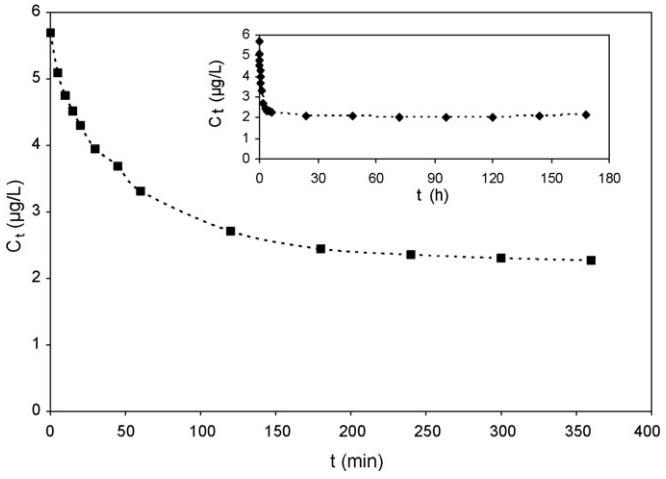

Fig. 2. Example of raw kinetics data for Bromacil adsorption in buffered water (pH 7.8) on PAC Norit SA-UF (# 21, C_0 = 5.7 μg L^{-1} and m_s = 0.3 mg L^{-1}).

Table 3
The classical kinetic models tested in this study (other models used are presented in the text).

Kinetic model	Rate equation		Linear form		Plot
External diffusion models					
Mass transfer classical model	$-\frac{dC_t}{dt} = k\left(\frac{a}{V}\right)(C_t - C_e)$	(1)	$\ln\left[\frac{C_0 - C_e}{C_t - C_e}\right] = k\left(\frac{a}{V}\right)t = k't$	(1 bis)	$\ln\left[\frac{C_0-C_e}{C_t-C_e}\right]$ vs t
Furusawa and Smith model [4]	$\frac{C_t}{C_0} = \frac{1}{1+m_sK_L} + \left[\frac{m_sK_L}{1+m_sK_L}\right]\exp\left[-\frac{(1+m_sK_L)k_fS_st}{m_sK_L}\right]$	(2)	$\ln\left[\frac{C_t}{C_0} - \frac{A}{m_sK_L}\right] = -\frac{k_fS_st}{A} + \ln A$ avec $A = \frac{m_sK_L}{1+m_sK_L}$	(2 bis)	$\ln\left[\frac{C_t}{C_0} - \frac{A}{m_sK_L}\right]$ vs t
Intra-particular diffusion models					
Weber and Morris model [6]	$q_t = \left(\frac{V}{m}\right)k_Wt^{1/2}$	(3)			q_t vs $t^{1/2}$
Vermeulen model [14]	$F_t = \left[1 - \exp\left(\frac{-\pi^2Dt}{R_a{}^2}\right)\right]^{1/2}$	(4)	$\ln\left[\frac{1}{1-F_t{}^2}\right] = \frac{\pi^2Dt}{R_a{}^2}$	(4 bis)	$\ln\left[\frac{1}{1-F_t{}^2}\right]$ vs t
Surface reaction models					
Pseudo-first-order model	$+\frac{dq_t}{dt} = k_{1app}(q_e - q_t)$	(5)	$\ln(q_e - q_t) = \ln(q_e) - k_{1app}t$	(5 bis)	$\ln(q_e - q_t)$ vs t
Pseudo-second-order model	$+\frac{dq_t}{dt} = k_{2app}(q_e - q_t)^2$	(6)	$\left(\frac{t}{q_t}\right) = \left(\frac{1}{k_{2app}q_e{}^2}\right) + \left(\frac{1}{q_e}\right)t$	(6 bis)	$\frac{t}{q_t}$ vs t

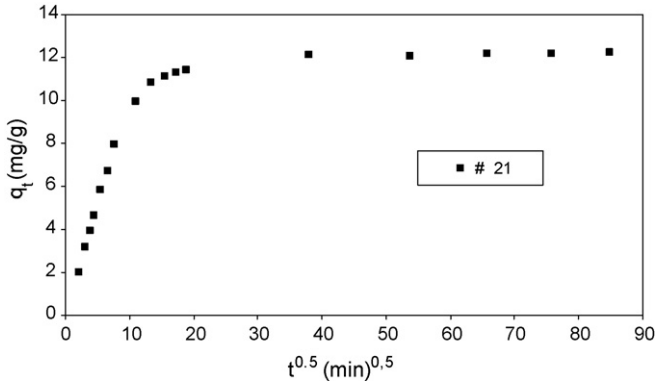

Fig. 3. Sorption kinetic governed by intra-particle diffusion. Application of a simplified Weber and Morris model (Eq. (3)) for Bromacil adsorption on PAC Norit SA-UF, at pH 7.8 (# 21; $0 < F_t < 1$).

The Weber and Morris model [6] is based on older studies, particularly those of Boyd et al. [13], founded on a theoretical approach developed for spherical adsorbent particles. Simplifications of this approach have been proposed in the literature, first by Vermeulen [14], Eq. (4) (Table 3), and recently reviewed in the literature [9,22,33]. The Vermeulen model was very suitable when applied to all of our results to $F_t = 0.8$–0.9 (with $R_a = 3\,\mu m$, radius of solid adsorbent assumed to be spherical). It should be noted, however, that the best linear correlation is not always an ordinate at origin zero. An example is presented in Fig. 4. The calculated diffusivity D values (Table 4) were all fairly similar, ranging from 0.2×10^{-15} to $1.5 \times 10^{-15}\ m^2\ s^{-1}$. There was no consistent significant effect of the equilibrium concentration (C_e). However, for ratios $C_e/C_0 \geq 0.5$, the D value was much more constant: $D_{average} = (0.4 \pm 0.09) \times 10^{-15}\ m^2\ s^{-1}$.

According to the results of a more recent study [22], the diffusivity D of the Vermeulen model is not constant and depends on the C_t value:

$$D = D_0[1 + (K_LC_t)^n]$$

with K_L and n Tóth isotherm constants, D_0, diffusivity independent of the adsorbate concentration.

Considering this D function and the Vermeulen model, the authors of this report [22] developed two new models, for the values

Table 4
Application of models of intra-particular diffusion (Eqs. (4) and (7)) for adsorption of Bromacil on PAC Norit SA-UF at pH 7.8.

Experiment	C_e ($\mu g\,L^{-1}$)	Model of Vermeulen (Eq. (4))				Model of Rudzinski and Plazinski (Eq. (7))[a]		
		$F_{t\,final}$[b]	r^2	$k_v\ (s^{-1}) = (\pi^2 \times D/R_a{}^2)$	$D\ (m^2\ s^{-1})$	$F_{t\,final}$[b]	r^2	$D_0\ (m^2\ s^{-1})$
# 1	247.8	0.80	0.968	0.5×10^{-3}	0.4×10^{-15}	0.85	0.956	1.1×10^{-16}
# 2	216	0.82	0.987	0.6×10^{-3}	0.5×10^{-15}	0.80	0.994	1.0×10^{-16}
# 3	205	0.80	0.956	0.6×10^{-3}	0.5×10^{-15}	0.80	0.972	1.1×10^{-16}
# 4	176	0.82	0.980	0.4×10^{-3}	0.4×10^{-15}	0.80	0.955	0.7×10^{-16}
# 5	115.5	0.80	0.93	0.5×10^{-3}	0.4×10^{-15}	0.80	0.986	1.2×10^{-16}
# 6	115	0.80	0.992	1.0×10^{-3}	0.9×10^{-15}	0.80	0.992	2.1×10^{-16}
# 7	94	0.80	0.977	0.5×10^{-3}	0.4×10^{-15}	0.80	0.983	1.3×10^{-16}
# 8	74	0.90	0.996	1.0×10^{-3}	0.9×10^{-15}	0.85	0.930	2.9×10^{-16}
# 9	67	0.83	0.930	0.7×10^{-3}	0.6×10^{-15}	0.85	0.922	2.2×10^{-16}
# 10	59	0.85	0.993	1.0×10^{-3}	0.9×10^{-15}	0.80	0.990	2.7×10^{-16}
# 11	57.5	0.65	0.967	0.3×10^{-3}	0.3×10^{-15}	0.65	0.982	1.0×10^{-16}
# 12	40	0.80	0.973	0.8×10^{-3}	0.7×10^{-15}	0.80	0.966	2.9×10^{-16}
# 13	28	0.80	0.963	0.9×10^{-3}	0.8×10^{-15}	0.80	0.962	3.6×10^{-16}
# 14	23	0.83	0.994	0.2×10^{-3}	0.2×10^{-15}	0.80	0.942	0.7×10^{-16}
# 16	15.6	0.85	0.990	0.7×10^{-3}	0.6×10^{-15}	0.85	0.984	2.7×10^{-16}
# 17	12.5	0.83	0.988	1.0×10^{-3}	0.9×10^{-15}	0.85	0.985	4.0×10^{-16}
# 18	5.3	0.87	0.971	1.6×10^{-3}	1.5×10^{-15}	0.85	0.960	6.8×10^{-16}
# 21	2.1	0.91	0.998	0.1×10^{-3}	0.9×10^{-15}	0.90	0.990	0.2×10^{-16}
# 22	2.0	0.90	0.996	1.4×10^{-3}	1.3×10^{-15}	0.85	0.987	0.9×10^{-16}

[a] $12.5\,\mu g\,L^{-1} < C_e < 247.8\,\mu g\,L^{-1}$: Eq. (7) with $K_{L(Toth)} = 10.2\,L\,mg^{-1}$ and $n_{Toth} = 0.82$; $2.0\,\mu g\,L^{-1} < C_e < 5.3\,\mu g\,L^{-1}$: Eq. (7) with $K_{L(Toth)} = 1089\,L\,mg^{-1}$ and $n_{Toth} = 0.82$.
[b] Application field: $0 < F_t < F_{t\,final}$.

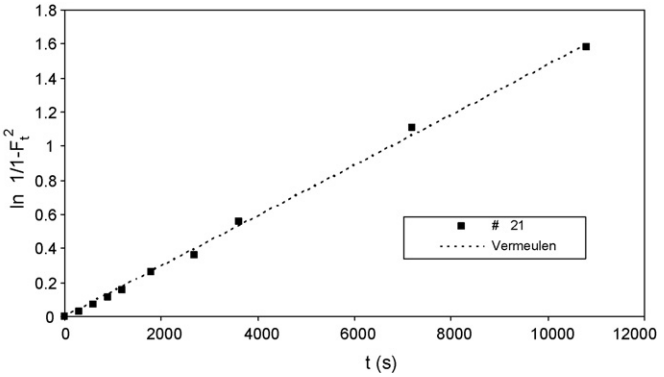

Fig. 4. Sorption kinetic governed by intra-particle diffusion. Application of Vermeulen model (Eq. (4)) for Bromacil adsorption on PAC Norit SA-UF, at pH 7.8 (# 21; $0 < F_t < 0.8–0.9$).

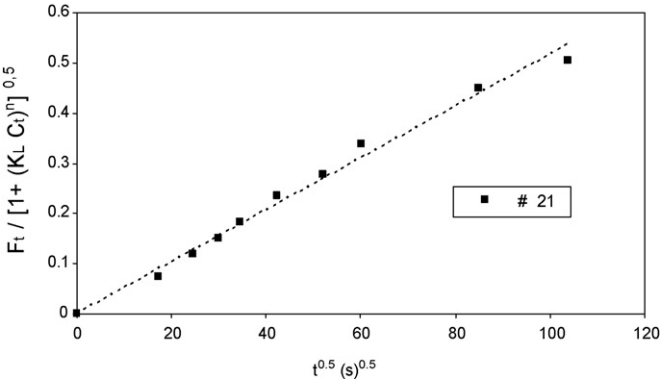

Fig. 5. Sorption kinetic governed by intra-particle diffusion. Application of Eq. (7) (with $R_a = 3$ μm, $K_L = 1089$, $n = 0.82$) for Bromacil adsorption on PAC Norit SA-UF at pH 7.8 (# 21; $0 < F_t < 0.85$).

of $F_t < \sim 0.3$ and $F_t > \sim 0.3$:

$$\frac{F_t}{[1+(K_L C_t)^n]^{1/2}} = \frac{6}{R_a}\left[\left(\frac{D_0}{\pi}\right)t\right]^{1/2} \quad (7)$$

$$\frac{\ln[\pi^2/6(1-F_t)]}{\pi^2}[1+(K_L C_t)^n] = -\frac{D_0 t}{{R_a}^2} \quad (8)$$

Only Eq. (7) suitably applied to our data (*via* the origin), for $F_t = 0.8–0.9$ and with Tóth parameters, K_L and n, determined elsewhere [28]. An example is presented in Fig. 5 and the D_0 values are given in Table 4.

In terms of thermodynamics, this expression is far more applicable than that of Vermeulen, since it takes the C_t value into account of which is a variable relative to one of the reaction reagents; with the other reagent being the available sites related to the F_t value.

As for the Vermeulen diffusivity, D_0 values became significantly constant for $C_e/C_0 \geq 0.5$: $D_{0\ \text{average}} = (1.0 \pm 0.2) \times 10^{-16}\ \text{m}^2\ \text{s}^{-1}$.

3.2.3. HSDM model

Based on the assumption that the adsorbent particles are identical, Mathews and Weber [15] proposed a model that has received much attention over the last two decades. This kinetic model, called the "homogeneous solid phase diffusion model" is based on the fact that the overall adsorption reaction is kinetically limited by external and homogeneous diffusion steps in the adsorbent. Other authors have called this model the "homogeneous surface diffusion model" with the main hypothesis being that the intra-particle diffusion phenomenon has two components: diffusion in the liquid within pores and diffusion on the pore surface, which is crucial for strongly adsorbable compounds [34,35]. Thus it has been demonstrated, based on the Fick law and digital algorithms, that the following kinetic law [35] applied regardless of the reactor:

$$\ln t^* = A_0 + A_1 C_t^* + A_2 (C_t^*)^2 + A_3 (C_t^*)^3 + \cdots = X \quad (9)$$

Parameters t^* and C^* are dimensionless relative to the reaction time and adsorbate concentration in the liquid phase, respectively. Parameters $A_0, A_1, A_2, \ldots$ describe the mathematical solution for a batch reactor and depend, in all cases, on the Freundlich constant n (characteristic of the adsorbate/adsorbent couple), and the Biot number Bi (physical characteristic of the adsorbent and the reactor) when the external diffusion step is also considered. The parameters A_i values are given in the literature [35] for different n and Bi values.

$$t* = \frac{tD_s}{R_a^2} \quad \text{and} \quad C* = \frac{C_t - C_e}{C_0 - C_e}$$

where t, real-time (s); D_s, surface diffusion coefficient ($\text{m}^2\ \text{s}^{-1}$); R_a, adsorbent particle radius (m); C_t, C_e, C_0, adsorbate concentrations (mg L^{-1} or mol L^{-1}).

The ln t *vs* X plot allows verification of the kinetic law and to determine D_s. This model is sometimes used to interpret batch results [2,3], but it is primarily used to model systems operating continuously, such as PAC/membrane [36–38] or granular activated carbon filtration [39–42] systems.

However, the conditions for applying the HSDM approach are restrictive [35], notably on the C_e/C_0 ratio which must be within the 0.45–0.56 range for an $n_{\text{Freundlich}}$ value of 0.6, for example. In the experiments presented in Table 1, only five of them (# 3, 4, 7, 9, 13) fulfilled these conditions, including the C_e/C_0 ratio, and three others did not deviate much from these conditions (# 2, 15, 21). An example of this application is presented in Fig. 6 and all the results are given in Table 5.

The model correctly applied, regardless of the $n_{\text{Freundlich}}$ value, which seemed to have little effect on the model application and on the values of the surface diffusion coefficient D_s values. Indeed, it was verified that the $n = 0.5$ value, when applied to all of the selected experiments (including # 21), had very little or no effect

Table 5
Application of HSDM model (Eq. (9)) for adsorption of Bromacil on PAC Norit SA-UF at pH 7.8.

Experiment	C_e ($\mu\text{g L}^{-1}$)	C_0 ($\mu\text{g L}^{-1}$)	C_e/C_0	HSDM approach (Eq. (9))			
				$F_{t\,\text{final}}$[a]	r^2	$n_{\text{Freundlich}}$	D_s ($\text{m}^2\ \text{s}^{-1}$)
# 2	216	351	0.61	0.97	0.976	0.6	4.5×10^{-16}
# 3	205	400	0.51	0.97	0.977	0.6	4.6×10^{-16}
# 4	176	356	0.49	0.96	0.974	0.6	4.5×10^{-16}
# 7	94	169	0.56	0.98	0.977	0.6	1.7×10^{-16}
# 9	67	145	0.46	0.94	0.955	0.6	1.5×10^{-16}
# 13	28	61	0.46	0.95	0.948	0.6	0.2×10^{-16}
# 15	17	30	0.57	0.72	0.946	0.6	0.08×10^{-16}
# 21	2	5.7	0.35	0.93	0.993	0.2	1.7×10^{-16}

[a] Application field: $0 < F_t < F_{t\,\text{final}}$.

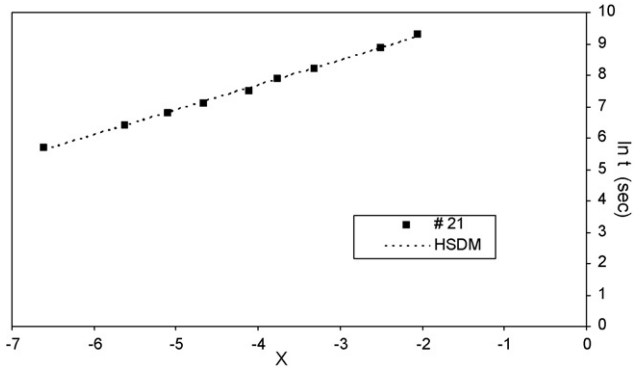

Fig. 6. Sorption kinetic governed by intra-particle diffusion. Application of HSDM approach (Eq. (9)) for Bromacil adsorption on PAC Norit SA-UF at pH 7.8 (# 21; $0 < F_t < 0.93$, $n = 0.2$).

on the D_s values. Note that the D_s value decreased sharply as C_0 or C_e decreased (Table 5), except at very low concentrations (# 21, $C_e = 2\ \mu g\ L^{-1}$) where the value obtained did not decline in the same way as in the other experiments ($17\ \mu g\ L^{-1} \le C_e \le 216\ \mu g\ L^{-1}$).

3.3. Adsorption kinetics governed by the surface reaction

The sorption reaction of a solute (or adsorbate) in solution on an adsorbent (or solid) to give rise to surface complexes between the solute and solid can be generally represented as follows:

$$(\text{FREE SITES})_{\text{solid}} + (\text{SOLUTE})_{\text{liquid or gas}} \underset{\text{desorption}}{\overset{\text{adsorption}}{\rightleftarrows}} (\text{COMPLEX})_{\text{solid}}$$

At t = 0		
q_m or q_e	C_0	0
At t > 0		
$(q_m - q_t)$ or $(q_e - q_t)$	C_t	q_t

Overall, the kinetic expression of this reaction should be based, as for all physicochemical equilibriums, on a combination of spontaneous adsorption reactions (rate constant k_{ads}) and reverse desorption reactions (k_{des}), with the two rate constants linked *via* the equilibrium constant (or K_L).

According to the literature [17], the surface reaction can be represented by a kinetic of $(n+1)$th global order (1st partial order in relation to the adsorbate in the liquid phase and nth partial order related to free sites on the adsorbent), and for desorption by a kinetic of nth order in relation to the complexed sites on the adsorbent, often called Langmuir kinetic equation:

$$+\frac{d\theta_t}{dt} = k_{ads}(1-\theta_t)^n C_t - k_{des}\,\theta_t{}^n \quad \text{with}\ \theta_t = \frac{q_t}{q_m} \tag{10}$$

This Langmuir model is applied when the adsorption kinetics is governed by the rate of surface reactions and it gives kinetic parameters for both adsorption and desorption simultaneous by using the data obtained from the adsorption experiment [43]. However, among the most commonly used models, the pseudo-first-order kinetic expression that neglects the desorption reaction, known as the Lagergren model [16], is usually mentioned, Eq. (5). The Lagergren empirical equation has also called pseudo-first-order kinetic equation because it was intuitively associated with the model of one-site-occupancy adsorption kinetics governed by the rate of surface reaction. The k_{1app} value will be a combination of adsorption k_{ads} and desorption k_{des} rate constants. This model did not perfectly fit our results, which is not surprising since its linear expression, Eq. (5 bis), is in the same form as the conventional external diffusion model. Moreover, in 2004, a purely mathematical interpretation [45] explains the suitable applicability of the pseudo-first-order model, demonstrating that it is identical to Langmuir model (Eq. (10) with $n = 1$) for the values of C_e close to C_0 (or q_t very low as compared to C_0). In our case, we cannot make this assumption.

The expression of pseudo-second-order, also very often used [17–20], is given Eq. (6) (Table 2). Its integration can lead to five possible forms which were all tested in this work. It is the linear expression Eq. (6 bis) (Table 2), which presents the best results (in terms of coefficient of linear regression and comparing calculated and experimental q_e), as shown by a lot of other authors [17,19,20]. An example is presented in Fig. 7 and values of k_{2app}, $q_{e(calc)}$ and ratio $q_{e(calc)}/q_{e(exp)}$ are given in Table 6.

This almost perfect application of the pseudo-second-order model may seem strange *a priori* from a thermodynamics standpoint, since only the concentration of available sites $(q_e - q_t)$ is taken into account in this model. However, as

$$q_t = \frac{C_0 - C_t}{m_s} \quad \text{and} \quad q_e = \frac{C_0 - C_e}{m_s}$$

Table 6
Application of pseudo-second-order model (Eq. (6)) for adsorption of Bromacil on PAC Norit SA-UF at pH 7.8, governed by surface reaction.

Experiment	C_e ($\mu g\ L^{-1}$)	C_0 ($\mu g\ L^{-1}$)	F_t[a]	r^2	$q_{e(calc)}$ ($mg\ g^{-1}$)	$q_{e(calc)}/q_{e(exp)}$	k_{2app} ($g\ mg^{-1}\ min$)	k_{2app}/m_s ($L\ mg^{-1}\ min^{-1}$)
# 1	248	361	0.90	0.986	133.3	1.17	0.3×10^{-3}	0.3
# 2	216	351	0.86	0.995	98.0	1.09	0.9×10^{-3}	0.6
# 3	205	400	0.90	0.998	101.0	1.04	1.1×10^{-3}	0.6
# 4	176	356	0.84	0.993	74.6	1.04	0.9×10^{-3}	0.4
# 6	115	371	0.85	0.999	88.5	1.03	2.2×10^{-3}	0.7
# 7	94	169	0.86	0.996	75.2	1.00	1.4×10^{-3}	1.4
# 8	74	320	0.90	0.999	69.9	1.15	1.8×10^{-3}	0.4
# 9	67	145	0.84	0.998	51.8	0.96	4.2×10^{-3}	2.9
# 10	59	158	0.84	0.998	59.9	1.12	2.5×10^{-3}	1.3
# 12	40	156	0.84	0.999	37.7	0.96	6.1×10^{-3}	2.0
# 14	23	31	0.85	0.972	29.5	0.98	1.4×10^{-3}	5.7
# 15	17.1	30	0.90	0.952	24.3	0.96	3.6×10^{-3}	7.1
# 16	15.6	53	0.85	0.996	16.6	1.11	6.5×10^{-3}	2.6
# 17	12.5	66	0.90	0.999	17.3	0.97	16.9×10^{-3}	5.6
# 18	5.3	38	0.90	0.995	18.0	1.10	8.4×10^{-3}	4.2
# 19	4.3	5.5	0.94	0.998	11.6	1.01	0.9×10^{-3}	8.6
# 20	2.9	5.4	0.91	0.997	12.6	1.03	0.9×10^{-3}	4.4
# 21	2.1	5.7	0.91	0.996	12.5	1.03	2.6×10^{-3}	8.8
# 22	2.0	30.8	0.90	0.999	10.9	1.13	17.5×10^{-3}	5.8
# 23	1.3	5.0	0.86	0.999	8.4	1.02	3.9×10^{-3}	9.9

[a] $F_{t\,final}$ (application field: $0 < F_t < F_{t\,final}$).

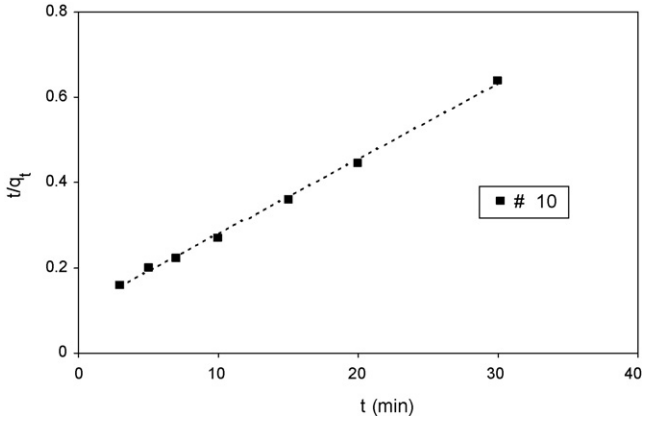

Fig. 7. Sorption kinetic governed by surface reactions. Application of pseudo-second order (Eq. (6 bis)) for Bromacil adsorption on PAC Norit SA-UF (# 10; $0 < F_t < 0.88$).

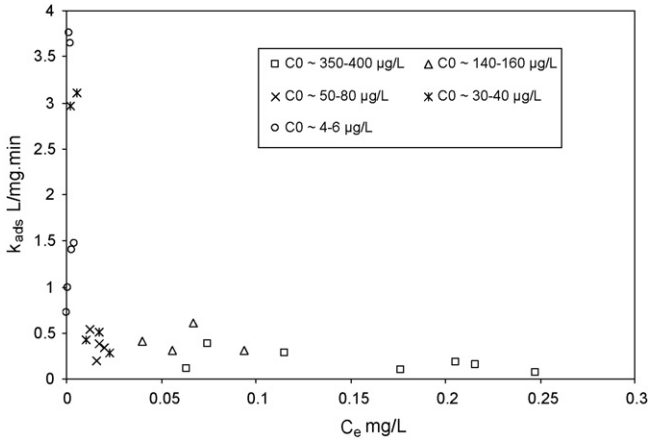

Fig. 8. Evolution of k_{ads} with C_e for Bromacil adsorption on PAC Norit SA-UF, governed by surface reaction.

Eq. (6) becomes more suitable for a reaction between two reagents, which in this study was the adsorbate, represented by $(C_t - C_e)$, and the adsorbent, represented by $(q_e - q_t)$.

$$+\frac{dq_t}{dt} = \frac{k_{2app}}{m_s}(C_t - C_e)(q_e - q_t) \quad (11)$$

The rate constant is then k_{2app}/m_s ($L\,mg^{-1}\,min^{-1}$). The obtained values are reported in Table 6.

There was a sharp increase in this latter constant as the equilibrium concentration C_e decreased.

The pseudo-second-order kinetic equation is a generalization of the Lagergren empirical equation for the two-sites-occupancy adsorption. A theoretical development of this equation based on applying the fundamental approach to kinetics of interfacial transport (Statistical Rate Theory) showed that this equation is a simplified form of a more general equation for the case when the adsorption kinetics is governed by the rate of surface reactions [44].

To explain the suitable applicability of the pseudo-second-order model, Azizian [45] showed that the kinetic so-called Langmuir model, i.e., Eq. (10) with $n = 1$, leads to an integrated expression similar to Eq. (6 bis) when the amount of adsorption is not very low.

This demonstration gave rise to the following relationship between k_{2app} and k_{ads}:

$$k_{2app} = -(b - \lambda)2q_e \quad (12)$$

with $\lambda = (b^2 - 4ac)^{0.5}$, where $b = -(\beta + C_0 + 1/K_L)k_{ads}$, $a = k_{ads}\beta$, $c = k_{ads}C_0$, $\beta = m_s q_m$, $K_L = k_{ads}/k_{des}$ (q_m and K_L are Langmuir equilibrium constants).

The k_{2app} value is then a complex function of C_0, k_{ads}, k_{des}, K_L and q_m (from Langmuir equilibrium and kinetic models). Some authors made mention that when the sorption data are well represented by pseudo-second-order kinetics for the entire reaction period, the sorption is controlled to chemisorption process [10,46,47].

The k_{ads} and k_{des} values calculated from k_{2app} are reported in Table 7. The data clearly show that the surface adsorption reaction rate was much higher for low C_e values than for high values (Fig. 8), while the opposite pattern was noted for the desorption rate.

Table 7
Kinetic constants k_{ads} and k_{des} calculated from pseudo-second-order constant k_{2app} (Eq. (6)) for adsorption of Bromacil on PAC Norit SA-UF at pH 7.8, governed by surface reaction.

Experiment	C_e ($\mu g\,L^{-1}$)	C_0 ($\mu g\,L^{-1}$)	k_{2app} ($g\,mg^{-1}\,min$)	k_{ads}[a] ($L\,mg^{-1}\,min^{-1}$)	k_{des}[a] (min^{-1})
# 1	248	361	0.3×10^{-3}	0.07	0.6×10^{-2}
# 2	216	351	0.9×10^{-3}	0.16	1.5×10^{-2}
# 3	205	400	1.1×10^{-3}	0.18	1.6×10^{-2}
# 4	176	356	0.9×10^{-3}	0.10	0.9×10^{-2}
# 6	115	371	2.2×10^{-3}	0.29	2.6×10^{-2}
# 7	94	169	1.4×10^{-3}	0.31	2.8×10^{-2}
# 8	74	320	1.8×10^{-3}	0.39	3.5×10^{-2}
# 9	67	145	4.2×10^{-3}	0.61	5.5×10^{-2}
# 10	59	158	2.5×10^{-3}	0.41	3.7×10^{-2}
# 12	40	156	6.1×10^{-3}	0.31	2.8×10^{-2}
# 14	23	31	1.4×10^{-3}	0.28	2.5×10^{-2}
# 15	17.1	30	3.6×10^{-3}	0.51	4.6×10^{-2}
# 16	15.6	53	6.5×10^{-3}	0.20	1.8×10^{-2}
# 17	12.5	66	16.9×10^{-3}	0.54	4.9×10^{-2}
# 18	5.3	38	8.4×10^{-3}	3.11	0.3×10^{-2}
# 19	4.3	5.5	0.9×10^{-3}	1.47	0.2×10^{-2}
# 20	2.9	5.4	0.9×10^{-3}	1.41	0.2×10^{-2}
# 21	2.1	5.7	2.6×10^{-3}	3.65	0.4×10^{-2}
# 22	2.0	30.8	17.5×10^{-3}	2.97	0.3×10^{-2}
# 23	1.3	5.0	3.9×10^{-3}	3.76	0.4×10^{-2}

[a] $12.5\,\mu g\,L^{-1} < C_e < 247.8\,\mu g\,L^{-1}$: Eq. (13) with $K_{L(Langmuir)} = 11\,L\,mg^{-1}$ and $q_{m(Langmuir)} = 151.5\,mg\,g^{-1}$ $1.3\,\mu g\,L^{-1} < C_e < 5.3\,\mu g\,L^{-1}$: Eq. (13) with $K_{L(Langmuir)} = 920\,L\,mg^{-1}$ and $q_{m(Langmuir)} = 18.1\,mg\,g^{-1}$.

4. Conclusion

Our study on Bromacil adsorption kinetics showed that many models are suitable, regardless of the considered step, i.e., intra-particle diffusion or surface reaction. It is therefore not possible to precisely specify *a priori* whether the diffusion or surface reaction is a key kinetic factor. The intra-particle diffusion models suitably fit the experimental results. However, the diffusivity D values of the Vermeulen model or the D_0 values of the Rudzinski and Plazinski model were only constant for values of the ratio $C_e/C_0 \geq 0.5$ ($D = (0.4 \pm 0.09) \times 10^{-15}$ and $D_0 = (1.0 \pm 0.2) \times 10^{-16}\ m^2\ s^{-1}$). The HSDM model also applied, but the surface diffusion coefficient (D_s) values were widely scattered (between 10^{-17} and $4 \times 10^{-16}\ m^2\ s^{-1}$) and decreased sharply with the initial or equilibrium Bromacil concentration.

The pseudo-second-order surface reaction model fit particularly well, which is logical since its integration led to a solution similar to that obtained with the integration of the Langmuir kinetic model. Some authors made mention that when the sorption data are well represented by such a kinetic model, the sorption is controlled to chemisorption process. In this latter case, for equilibrium concentrations over $\sim 10\ \mu g\ L^{-1}$, the adsorption and desorption constants were relatively independent of C_e ($k_{ads} = 0.31 \pm 0.16\ L\ mg^{-1}\ min^{-1}$ and $k_{des} = (2.8 \pm 1.4) \times 10^{-2}\ min^{-1}$). For equilibrium concentrations less than or equal to $10\ \mu g\ L^{-1}$, the adsorption constants were significantly higher ($k_{ads} = 2.73 \pm 0.95\ L\ mg^{-1}\ min^{-1}$) and the desorption constants were significantly lower ($k_{des} = (0.3 \pm 0.08) \times 10^{-2}\ min^{-1}$). This kinetic observation clearly confirmed the hypothesis based on two types of site put forward on the basis of the initial equilibrium adsorption study (part 1):

- highly reactive and weakly concentrated sites on the PAC surface ($K_{L(Langmuir)} \sim 1000\ L\ mg^{-1}$, $q_{m(Langmuir)} \sim 20\ mg\ g^{-1}$, $k_{ads} \sim 3\ L\ mg^{-1}\ min^{-1}$, $k_{des} \sim 3 \times 10^{-3}\ min^{-1}$);
- more numerous but more weakly reactive sites ($K_{L(Langmuir)} \sim 10\ L\ mg^{-1}$, $q_{m(Langmuir)} \sim 150\ mg\ g^{-1}$, $k_{ads} \sim 0.3\ L\ mg^{-1}\ min^{-1}$, $k_{des} \sim 3 \times 10^{-2}\ min^{-1}$).

Acknowledgments

This study was conducted at the Laboratory of Chemistry and Microbiology of Water (CNRS UMR 6008) of the Engineering Institute of Poitiers in the University of Poitiers in France with the financial support from the University of Damascus in Syria.

References

[1] D.R.U. Knappe, V.L. Snoeyink, Predicting the removal of atrazine by powdered and granular activated carbon—Final Report, Compagnie Générale des Eaux, 1995.
[2] G. McKay, Application of surface diffusion model to the adsorption of dyes on bagasse pith, Adsorption 4 (1998) 361–372.
[3] D. Cook, G. Newcombe, P. Sztajnbok, The application of PAC for MIB and Geosmin removal: predicting PAC doses in four raw waters, Water Research 35 (2001) 1325–1333.
[4] T. Furusawa, J.M. Smith, Fluid-particle and intraparticle mass transport rates in slurries, Industrial Engineering Chemical Fundamental 12 (1973) 197–203.
[5] G. McKay, Adsorption of dyestuffs from aqueous solutions with activated carbon IV: external mass transfer processes, Journal of Chemistry Technology Biotechnology 33 (1983) 205–218.
[6] J.R. Weber, J.C. Morris, Kinetics of adsorption on carbon from solution, Journal of Sanitary Engineering Division 89 (1963) 31–39.
[7] M. Sarkar, P.M. Acharya, B. Bhattacharya, Modeling the adsorption kinetics of some priority organic pollutants in water from diffusion and activation energy parameters, Journal of Colloid and Interface Science 266 (2003) 28–32.
[8] O. Hamdaoui, Batch study of liquid-phase adsorption of methylene blue using cedar sawdust and crushed brick, Hazardous Materials B135 (2006) 264–273.
[9] V.C. Srivastava, M.M. Swamy, D. Malli, B. Prasad, I.M. Mishra, Adsorptive removal of phenol by bagasse fly ash and activated carbon: equilibrium, kinetics and thermodynamics, Colloids and Surfaces A: Physicochemical and Engineering Aspects 272 (2006) 89–104.
[10] D. Karadag, Modeling the mechanism, equilibrium and kinetics for the adsorption of Acid Orange 8 onto surfactant-modified clinoptilolite: the application of nonlinear regression analysis, Journal of Dyes and Pigments 74 (2007) 659–664.
[11] B.H. Hameed, Equilibrium and kinetic studies of methyl violet sorption by agricultural waste, Journal of Hazardous Materials 154 (2007) 204–212.
[12] E.N. El Qada, S.J. Allen, G.M. Walker, Kinetic modeling of the adsorption of basic dyes onto steam-activated bituminous coal, Industrial and Engineering Chemistry Research 46 (2007) 4764–4771.
[13] G.E. Boyd, A.W. Adamson, L.S. Myres, Kinetics of ionic exchange adsorption processes, Journal of American Chemistry 69 (1947) 2836–2848.
[14] T. Vermeulen, Journal of Industrial and Engineering Chemistry 45 (1953) 1664–1670.
[15] A.P. Mathews, W.J. Weber, Effect of external mass transfer and intraparticule diffusion on adsorption rates in slurry reactors, Journal of Aiche Symposium Series 73 (1977) 91–98.
[16] S. Lagergren, K. Sven, Vetenskapsakad Handlingar 24 (1898) 1–5.
[17] Y.S. Ho, G. McKay, A Two-stage batch sorption optimized design for dye removal to minimize contact time, Process Safety Environment Protection 76 (1998) 313–318.
[18] G. Blanchard, M. Maunaye, G. Martin, Removal of heavy metals from waters by means of natural zeolites, Water Research 18 (1984) 1501–1507.
[19] Y.S. Ho, G. McKay, Pseudo-second order model for sorption processes, Process Biochemistry 34 (1999) 451–465.
[20] Y.S. Ho, G. McKay, The kinetics of sorption of divalent metal ions onto sphagnum moss peat, Water Research 34 (2000) 735–742.
[21] K.V. Kumar, Pseudo-second order models for the adsorption of safranine onto activated carbon: comparison of linear and non-linear regression methods, Journal of Hazardous Materials 142 (2007) 564–567.
[22] W. Rudzinski, W. Plazinski, Theoretical description of the kinetics of solute adsorption at heterogeneous solid/solution interfaces on the possibility of distinguishing between the diffusional and the surface reaction kinetics models, Journal of Applied Surface Science 253 (2007) 5827–5840.
[23] C. Aharoni, S. Sideman, E. Hoffer, Adsorption of phosphate ions by collodion-coated alumina, Journal of Chemical Technology Biotechnology 29 (1979) 404–412.
[24] C.A. Ward, R.D. Findlay, M. Rizk, Journal of Chemical Physics 76 (1981) 5599–5605.
[25] J.A.W. Elliott, C.A. Ward, W. Rudzinski, W.A. Steele, G. Zgrablich, Equilibrium and Dynamics of Gas Adsorption on Heterogeneous Solid Surfaces, Elsevier, Amsterdam, 1997.
[26] W. Rudzinski, T. Panczyk, Remarks on the current state of adsorption kinetic theories for heterogeneous solid surfaces: a comparison of the art and the SRT approaches, Langmuir 18 (2002) 439–449.
[27] W. Piasecki, Theoretical description of the kinetics of proton adsorption at the oxide/electrolyte interface based on the statistical rate theory of interfacial transport and the model of surface charging, Langmuir 19 (2003) 9526–9533.
[28] F. Al Mardini, B. Legube, Effect of the adsorbate (Bromacil) equilibrium concentration in water on its adsorption on powdered activated carbon. Part 1: Equilibrium parameters, Journal of Hazardous Materials, in press, doi:10.1016/j.jhazmat.2009.05.003.
[29] C. Campos, L. Schimmoller, B.J. Mariñas, V.L. Snoeyink, I. Baudin, J.-M. Laîné, Adding PAC to remove DOC, Journal of American Water Works Association 92 (2000) 69–83.
[30] Q. Li, V.L. Snoeyink, B.J. Mariñas, C. Campos, Pore blockage effect of NOM on atrazine adsorption kinetics of PAC: the roles of NOM molecular weight and PAC pore size distribution, Water Research 37 (2003) 4863–4872.
[31] Li Ding, B.J. Mariñas, L.C. Schideman, V.L. Snoeyink, Competitive effects of natural organic matter: parametrization and verification of the three-component adsorption model COMPSORB, Environmental Science and Technology 40 (2006) 350–356.
[32] Q. Li, V.L. Snoeyink, C. Campos, B.J. Mariñas, Displacement effect of NOM on atrazine adsorption by PACs with different pore size distributions, Environmental Science and Technology 36 (2002) 1510–1515.
[33] A. Kumar, S. Kumar, S. Kumar, D.V. Gupta, Adsorption of phenol and 4-nitrophenol on granular activated carbon in basal salt medium: equilibrium and kinetics, Journal of Hazardous Materials 147 (2007) 155–166.
[34] D.W. Hand, User-oriented solutions to the homogeneous surface diffusion model for adsorption process design calculations. Part I: Batch reactor solutions, Thesis presented to Michigan Technology University, 1982.
[35] D.W. Hand, J.C. Crittenden, M. Asce, W.E. Thacker, User-oriented batch reactors solutions to the homogeneous surface diffusion model, Journal of Environmental Engineering 109 (1983) 82–101.
[36] L. Li, P.A. Quinlivane, D.R.U. Knappe, Effects of activated carbon surface chemistry and pore structure on the adsorption of organic contaminants from aqueous solution, Journal of Carbon 40 (2002) 2085–2100.
[37] Q. Li, B.J. Mariñas, V.L. Snoeyink, C. Campos, Three-component competitive adsorption model for flow-through PAC systems. 1. Model development and verification with a PAC/membrane system, Environmental Science and Technology 37 (2003) 2997–3004.
[38] S. Chang, T.D. Waite, A.G. Fane, A simplified model for trace organics removal by continuous flow PAC adsorption/submerged membrane processes, Journal of Membrane Science 254 (2005) 81–87.
[39] I.M.C. Lo, P.A. Alok, Computer simulation of activated carbon adsorption for multi-component systems, Journal of the Environment International 22 (1996) 239–252.

[40] S. Baup, C. Jaffre, D. Wolbert, A. Laplanche, Adsorption of pesticides onto granular activated carbon: determination of surface diffusivities using simple batch experiments, Journal of Adsorption 6 (2000) 219–228.
[41] L.C. Schideman, B.J. Mariñas, V.L. Snoeyink, C. Campos, Three-component competitive adsorption model for fixed-bed and moving-bed granular activated carbon adsorbers. Part I: Model development, Journal of Environmental Science and Technology 40 (2006) 6805–6811.
[42] L.C. Schideman, V.L. Snoeyink, B.J. Mariñas, L. Ding, C. Campos, Application of a three-component competitive adsorption model to evaluate and optimize granular activated carbon systems, Journal of Water Research 40 (2007) 3289–3298.
[43] F.T. Lindstrom, R. Haque, W.R. Coshow, Adsorption solution. III. A new model for the kinetics of adsorption–desorption processes, Journal of Physical Chemistry 74 (1970) 495–503.
[44] W. Rudzinski, W. Plazinski, Kinetics of solute adsorption at solid/solution interfaces: a theoretical development of the empirical pseudo-first and pseudo-second order kinetic rate equations, based on applying the statistical rate theory of interfacial transport, Journal of Physical Chemistry B 110 (2006) 16514–16525.
[45] S. Azizian, Kinetic models of sorption: a theoretical analysis, Journal of Colloid and Interface Science 267 (2004) 47–52.
[46] K.V. Kumar, V. Ramamurthi, S. Sivanesan, Modeling the mechanism involved during the sorption of methylene blue onto fly ash, Journal of Colloid and Interface Science 284 (2005) 14–21.
[47] F. Banat, A.A. Sameer, A.M. Leema, Utilization of raw and activated date pits for the removal of phenol from aqueous solution, Chemical Engineering and Technology 27 (2004) 80–86.